

Non-perturbative evaluation of c_{SW} for smeared link clover fermion and Iwasaki gauge action

Yusuke Taniguchi*

Graduate School of Pure and Applied Sciences, University of Tsukuba,

Tsukuba, Ibaraki 305-8571, Japan

E-mail: taniguchi@het.ph.tsukuba.ac.jp

We performed a rough estimate of the non-perturbative value of the clover term coefficient c_{SW} for the APE stout link Wilson fermion. We varied the number of smearings from $N_{\text{smear}} = 1$ to 6 and adopted β values roughly corresponding to the lattice spacing of 0.1 fm. We used the Schrödinger functional technique for an evaluation of c_{SW} and found that c_{SW} decreases monotonically as we increase N_{smear} but has a 10% order of deviation from the tree level value for $N_{\text{smear}} = 6$.

The 30th International Symposium on Lattice Field Theory

June 24 - 29, 2012

Cairns, Australia

*Speaker.

1. Introduction

The $O(a)$ improved Wilson fermion with the smeared link variable [1, 2] is shown to have several virtues compared with the thin link fermion; a better scaling behavior, a fewer exceptional configuration [3] and a better chiral behavior [4, 5].

The improvement factor c_{SW} for the clover term is expected to be smaller [6] than that for the unsmeared link action. The tree level tadpole improved value seems to be consistent with the non-perturbative value [7]. Moreover recent studies with highly smeared link action [5, 8] adopt the tree level value $c_{\text{SW}} = 1$.

In this proceeding we would like to confirm if and how the non-perturbative value of c_{SW} is close to unity. We are also interested in the behavior of c_{SW} as we increase the number of smearings by fixing the lattice spacing. For this purpose we tried to set β to correspond to the lattice spacing $a = 0.1$ fm.

2. Schrödinger functional scheme

For an evaluation of c_{SW} we make use of the well established Schrödinger functional technique [9]. In this method we measure four kinds of two point functions between the axial current A_0 or the pseudo scalar density P in the bulk and the “pseudo scalar density” $O(t=0)$ or $O'(t=T)$ at the temporal boundary

$$f_A(x_0) = -\frac{1}{N_f^2 - 1} \langle A_0^a(x_0) O^a \rangle, \quad f_P(x_0) = -\frac{1}{N_f^2 - 1} \langle P^a(x_0) O^a \rangle, \quad (2.1)$$

$$f'_A(x_0) = +\frac{1}{N_f^2 - 1} \langle A_0^a(T - x_0) O'^a \rangle, \quad f'_P(x_0) = -\frac{1}{N_f^2 - 1} \langle P^a(T - x_0) O'^a \rangle. \quad (2.2)$$

The PCAC quark masses are defined in terms of the improved current

$$m(x_0) = r(x_0) + c_A s(x_0), \quad m'(x_0) = r'(x_0) + c_A s'(x_0), \quad (2.3)$$

$$r(x_0) = \frac{(\partial_0 + \partial_0^*) f_A(x_0)}{4f_P(x_0)}, \quad s(x_0) = \frac{a\partial_0\partial_0^* f_P(x_0)}{2f_P(x_0)}, \quad (2.4)$$

$$r'(x_0) = \frac{(\partial_0 + \partial_0^*) f'_A(x_0)}{4f'_P(x_0)}, \quad s'(x_0) = \frac{a\partial_0\partial_0^* f'_P(x_0)}{2f'_P(x_0)}. \quad (2.5)$$

The improved factor c_A for the axial current can be removed by adding an $O(a^2)$ term

$$M(x_0, y_0) = m(x_0) - \frac{m(y_0) - m'(y_0)}{s(y_0) - s'(y_0)} s(x_0) = r(x_0) - \frac{r(y_0) - r'(y_0)}{s(y_0) - s'(y_0)} s(x_0), \quad (2.6)$$

$$M'(x_0, y_0) = m'(x_0) - \frac{m'(y_0) - m(y_0)}{s'(y_0) - s(y_0)} s'(x_0) = r'(x_0) - \frac{r'(y_0) - r(y_0)}{s'(y_0) - s(y_0)} s'(x_0). \quad (2.7)$$

The massless limit is given by tuning the hopping parameter so that

$$M\left(\frac{T}{2}, \frac{T}{4}\right) \rightarrow 0 \quad (2.8)$$

and the non-perturbative c_{SW} is given by the improvement condition

$$\Delta M = M\left(\frac{3T}{4}, \frac{T}{4}\right) - M'\left(\frac{3T}{4}, \frac{T}{4}\right) \rightarrow 0 \quad (2.9)$$

with the hopping parameter set to its critical value κ_c .

3. Simulation setups

We adopt the Iwasaki gauge action and the improved Wilson fermion action with the clover term. The number of flavors is set to $N_f = 3$ with degenerate masses, which shall be tuned to zero. The APE stout smeared gauge link is used for those in the fermion action including the clover term. The smearing parameter is set to $\rho = 0.1$ [1]. We vary the number of smearings from one to six. We adopt $8^3 \times 16$ lattice with the Schrödinger functional boundary condition in the temporal direction [9].

The gauge coupling β is tuned so that the lattice spacing becomes around 0.1 fm. Since we would like to know a rough tendency of the improvement parameter c_{SW} we fix β just by guess except for that at $N_{\text{smear}} = 6$. The simulation parameter β is given in table 1 for each N_{smear} together with the inverse lattice spacing in the unit of GeV. The inverse lattice spacing is measured on $24^3 \times 48$ lattice by using the Sommer scale r_0 for $N_{\text{smear}} = 1, 2, 3$ at unphysically heavy quark masses $m_\pi > 500$ MeV. Those at $N_{\text{smear}} = 4, 6$ are measured at the physical quark mass with the Ω baryon mass input.

The non-perturbative c_{SW} was not necessarily adopted for the measurement of a^{-1} . The c_{SW} used for the measurement is given in the fourth column of the table 1. As can be seen from the data at $N_{\text{smear}} = 6$ the inverse lattice spacing a^{-1} has a tendency to grow up when we increase c_{SW} . The inverse lattice spacing given by r_0 also increase when we approach the physical quark mass point. a^{-1} at $N_{\text{smear}} = 1 - 4$ would appear to be larger than 2 GeV with the non-perturbative c_{SW} at the physical quark mass.

Table 1: Number of smearings and β for numerical simulation. The third column is a rough estimate of the lattice spacing measured with c_{SW} given in the fourth column. The data for $N_{\text{smear}} = 0$ is taken from Ref. [10].

N_{smear}	β	a^{-1} (GeV)	c_{SW} for a^{-1}
0	1.90	2.194(10)	1.715
1	1.95	2.65	1.20
2	1.93	2.35	1.00
3	1.91	2.25	1.00
4	1.89	2.119(88)	1.00
6	1.87	2.073(19)	1.00
6	1.87	2.340(26)	1.10
6	1.82	2.044(38)	1.10
6	1.82	2.192(09)	1.13

4. Numerical results

A typical behavior of the PCAC mass M and the mass difference ΔM is plotted in figure 1 for $N_{\text{smear}} = 6$ and $\beta = 1.82$ at three values of c_{SW} . The PCAC mass difference ΔM (up triangle) tends to decrease as we increase c_{SW} and crosses zero around $c_{\text{SW}} = 1.1$.

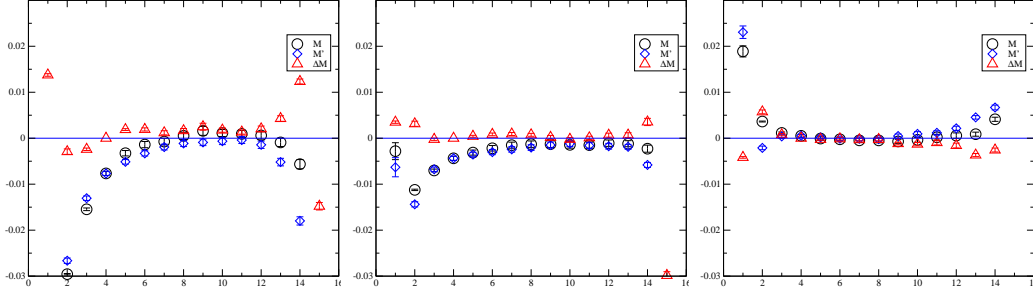


Figure 1: The PCAC mass $M(x_0, y_0)$, $M'(x_0, y_0)$ and the mass difference $\Delta M(x_0, y_0)$ as a function of x_0 for $N_{\text{smear}} = 6$, $\beta = 1.82$. y_0 is set to $T/4$. Three values of c_{SW} are adopted: 1.0 (left), 1.1 (middle) and 1.2 (right). The PCAC mass is tuned to be consistent with zero at $x_0 = T/2$.

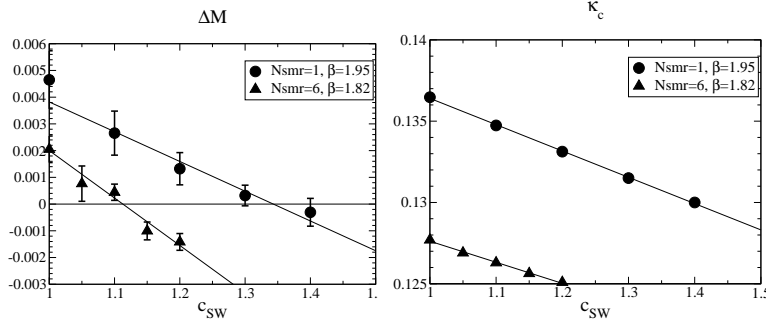


Figure 2: The PCAC mass difference $\Delta M(3/4T, T/4)$ (left) and the critical hopping parameter κ_c (right) as a function of c_{SW} . Two data are plotted with $N_{\text{smear}} = 1$ (circle) and 6 (triangle).

We plot this behavior in the left panel of figure 2 for $N_{\text{smear}} = 1$ and 6. Both data can be fitted by a linear function. The horizontal value where ΔM crosses zero is the non-perturbative c_{SW} . The linear fit works well for other N_{smear} and the result is listed in table 2.

Since the hopping parameter is tuned so that the PCAC mass is consistent with zero it represents the critical κ_c at each c_{SW} . κ_c can also be fitted linearly as a function of c_{SW} as is shown in the right panel of figure 2. The value of κ_c at the non-perturbative c_{SW} is listed in table 2 for each N_{smear} .

The non-perturbative c_{SW} is plotted as a function of number of smearings in the left panel of figure 3. c_{SW} decreases monotonically as a function of N_{smear} . We found roughly a 10% order of deviation from the tree level value even at $N_{\text{smear}} = 6$. The critical hopping parameter κ_c is also given in the right panel of figure 3. The decreasing behavior is almost the same as that of c_{SW} as a function of the number of smearings. κ_c is very near to the tree level value $1/8$ at $N_{\text{smear}} = 6$, which is one of the evidences of the good chiral behavior of the smeared link action.

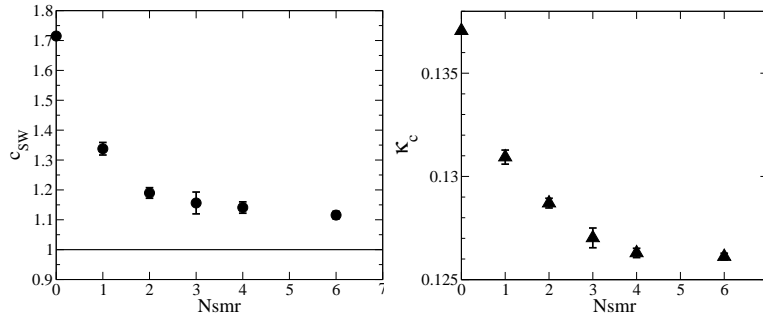
From (2.6) and (2.7) a quantity

$$c'_A(x_0) = -\frac{r(x_0) - r'(x_0)}{s(x_0) - s'(x_0)} \quad (4.1)$$

plays a role of the improvement coefficient of the axial vector current. As can be seen from figure

Table 2: The result for the non-perturbative c_{SW} and the critical hopping parameter κ_c . The data for $N_{\text{smear}} = 0$ is taken from Ref. [10].

N_{smear}	β	c_{SW}	κ_c
0	1.90	1.715	0.13706
1	1.95	1.342(21)	0.13094(34)
2	1.93	1.187(18)	0.12871(24)
3	1.91	1.155(43)	0.12702(48)
4	1.89	1.137(19)	0.12629(23)
6	1.87	1.057(20)	0.12634(22)
6	1.82	1.1127(96)	0.12612(16)

**Figure 3:** The non-perturbative c_{SW} (left panel) and the critical hopping parameter κ_c (right panel) as a function of the number of smearings.

4 x_0 dependence of c'_A is very flat near the non-perturbative c_{SW} and we are able to define the improvement factor of the axial current by

$$c_A = c'_A \left(\frac{T}{4} \right). \quad (4.2)$$

This c_A is fitted linearly as a function of c_{SW} as is shown in figure 5. We evaluate c_A at the non-perturbative c_{SW} and adopt it as its non-perturbative value. The results are plotted in figure 6 for each N_{smear} , which turned out to be very small and are consistent with zero within the statistical error.

5. Conclusion

We evaluate the non-perturbative value of the improvement coefficient c_{SW} of the clover term for the APE smeared link fermion action. We adopted $N_{\text{smear}} = 1 - 6$ as the number of smearings. The bare coupling β is tuned so that the lattice spacing is near to $a \sim 0.1$ fm as possible. The result is given in table 2 and figure 3. c_{SW} decreases smoothly as we increase the number of smearings. However we found a 10% deviation from the tree level value even at $N_{\text{smear}} = 6$.

As a byproduct we also evaluate the improvement factor c_A of the axial current, which turned out to be consistent with zero within the statistical error.

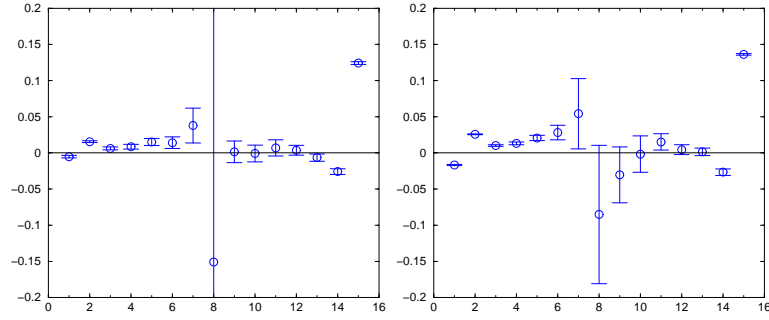


Figure 4: The axial current improvement factor c'_A as a function of x_0 . The c_{SW} is set to be nearest to the non-perturbative value. The left panel is $N_{\text{smeared}} = 1$, $c_{\text{SW}} = 1.3$. The right panel is $N_{\text{smeared}} = 6$, $c_{\text{SW}} = 1.1$. The hopping parameter is set to κ_c .

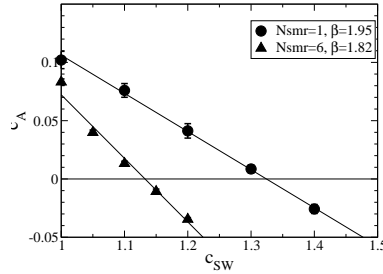


Figure 5: The improvement factor c_A as a function of c_{SW} . Two data are plotted with $N_{\text{smeared}} = 1$ (circle) and 6 (triangle).

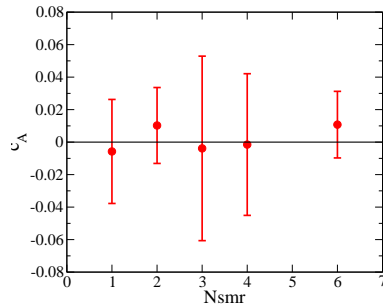


Figure 6: The non-perturbative improvement factor c_A as a function of the number of smearings N_{smeared} . All the data are consistent with zero within the statistical error.

Acknowledgement

This work is supported in part by Grants-in-Aid of the Ministry of Education (Nos. 22540265, 23105701).

References

- [1] C. Morningstar and M. J. Peardon, Phys. Rev. D **69**, 054501 (2004) [hep-lat/0311018].

- [2] S. Capitani, S. Durr and C. Hoelbling, JHEP **0611**, 028 (2006) [hep-lat/0607006].
- [3] S. Durr, Z. Fodor, C. Hoelbling, R. Hoffmann, S. D. Katz, S. Krieg, T. Kurth and L. Lellouch *et al.*, Phys. Rev. D **79**, 014501 (2009) [arXiv:0802.2706 [hep-lat]].
- [4] S. Capitani, S. Durr and C. Hoelbling, PoS LAT **2006**, 157 (2006) [hep-lat/0609059].
- [5] S. Durr, Z. Fodor, C. Hoelbling, S. D. Katz, S. Krieg, T. Kurth, L. Lellouch and T. Lippert *et al.*, Phys. Lett. B **705**, 477 (2011) [arXiv:1106.3230 [hep-lat]].
- [6] R. Horsley, H. Perlt, A. Schiller, P. E. L. Rakow and G. Schierholz, PoS LAT **2007**, 250 (2007) [arXiv:0710.0990 [hep-lat]].
- [7] R. G. Edwards, B. Joo and H. -W. Lin, Phys. Rev. D **78**, 054501 (2008) [arXiv:0803.3960 [hep-lat]].
- [8] S. Durr, Z. Fodor, C. Hoelbling, S. D. Katz, S. Krieg, T. Kurth, L. Lellouch and T. Lippert *et al.*, Phys. Lett. B **701**, 265 (2011) [arXiv:1011.2403 [hep-lat]].
- [9] M. Luscher, S. Sint, R. Sommer, P. Weisz and U. Wolff, Nucl. Phys. B **491** (1997) 323 [arXiv:hep-lat/9609035].
- [10] S. Aoki *et al.* [PACS-CS Collaboration], Phys. Rev. D **81**, 074503 (2010) [arXiv:0911.2561 [hep-lat]].